We are IntechOpen, the world's leading publisher of Open Access books Built by scientists, for scientists

4,800
Open access books available

122,000
International authors and editors

135M
Downloads

Our authors are among the

154
Countries delivered to

TOP 1%
most cited scientists

12.2%
Contributors from top 500 universities

WEB OF SCIENCE™

Selection of our books indexed in the Book Citation Index in Web of Science™ Core Collection (BKCI)

Interested in publishing with us?
Contact book.department@intechopen.com

Numbers displayed above are based on latest data collected.
For more information visit www.intechopen.com

Chapter 8

Thermal Conductivity Measurement of Vacuum Tight Dual-Edge Seal for the Thermal Performance Analysis of Triple Vacuum Glazing

Saim Memon

Additional information is available at the end of the chapter

http://dx.doi.org/10.5772/intechopen.74255

Abstract

A vacuum tight glass edge seal's thermal conductivity is one of the principal factor in determining the heat distribution towards the centre of pane, ultimately influences the thermal transmittance (U-value) of a triple vacuum glazing. So far indium and solder glass have proven to be vacuum tight edge sealing materials but both have certain limitations. In this chapter, a new low-temperature vacuum tight glass edge seal composite's thermal conductivity, Cerasolzer CS186 alloy and J-B Weld epoxy-steel resin, were measured and validated with the mild-steel and indium using transient plane source method with a sensor element of double spiral and resistance thermometer in a hot disk thermal constants analyser TPS2500s are reported. The thermal conductivity data of Cerasolzer CS186 alloy and J-B Weld epoxy steel resin were measured to be 46.49 and 7.47 $Wm^{-1} K^{-1}$, with the deviations (using analytical method) of ± 4 and $\pm 7\%$ respectively. These values were utilised to predict the thermal transmittance value of triple vacuum glazing using 3D finite element model. The simulated results show the centre-of-glass and total U-value of 300×300 mm triple vacuum glazing to be 0.33 and 1.05 $Wm^{-2} K^{-1}$, respectively. The influence of such a wide edge seal on the temperature loss spreading from the edge to the central glazing area is analysed, in which the predictions show wider edge seal has affected the centre-of-glass U-value to 0.043 $Wm^{-2} K^{-1}$ due to the temperature gradient loss spread to 54 and 84 mm on the cold and warm side respectively.

Keywords: thermal conductivity, transient plane source, triple vacuum glazing, thermal performance, vacuum seal

1. Introduction

Carbon reduction and energy efficiency of domestic buildings have been one of the major global concerns due to limits with climate change [1]. Energy efficiency can be improved by high performance smart windows, high levels of wall insulation, efficient appliances and effectiveness of renewable energy results in saving financial cost to consumers and carbon dioxide emissions [2, 3]. One of the main functions of a smart triple vacuum glazed windows is to reduce heat flow between indoors and outdoors, i.e. to provide preeminent thermal insulation so called thermal transmittance (U-value) [4]. It depends on the number of glass panes, the space between glass panes, emissivity of the coatings on glass pane, frame in which the glass is installed, the type of spacers that separate the panes of glass and the type of window frame. The total U-value includes the effect of the frame and the glazing edge area. An influence of the glazing edge area is dependent on the width and the type of edge sealing material.

The hermetic edge seal of a triple vacuum glazing must be capable of maintaining vacuum pressure of less than 0.1 Pa in order to suppress gaseous conduction for long term duration [5]. Sealing of two glass panes edges using high power laser through quartz window in vacuum chamber was developed by Benson et al. [6]. This achieves hermetic seal but the level of vacuum was not less than 0.1 Pa, due to gases and vapour particles caused by lasering remain in the cavity [7]. High temperature edge sealing technique developed by the Collins group at the University of Sydney is based on material solder glass sealed at high temperature around 450°C [8–10]. This technique achieved significant centre of pane U value of 0.8 $Wm^{-2}\,K^{-1}$ and considered at commercial level. The problems with high temperature method of sealing is degradation of low emittance coatings only hard coatings can be used, if using toughened glass then loss of toughness, and require more amount of heat energy for fabrication due to heat require for several hours. Low temperature solder glass material was investigated to form a hermetic edge seal, but durability was a problem due to the absorption of moisture. Polymers have problems of gas permeability and out gassing [7]. Low temperature edge sealing technique developed at the University of Ulster is based on Indium alloy sealed at low temperature process about 160°C. It requires secondary adhesive seal to prevent access from moisture [11, 12]. A low temperature sealing process allows the use of low emittance soft coatings reduces radiative heat transfer between glass panes and toughened glass allows to increase support pillar spacing reduces conductive heat transfer. The problem with low temperature edge sealing material is indium alloy is high-priced and for long term cost effective vacuum glazing, this method is not encouraged at commercial level [13, 14].

A new low-temperature composite materials and methods of fabrication was reported in Memon et al. [15]. In which CS-186 type of Cerasolzer and steel reinforced epoxy by J-B resin were used for the development of triple vacuum glazing as shown in **Figure 1**. In this chapter, the experimental measurements of thermal conductivity of this composite material are reported. The significance of this study is to analyse the influence of edge area on the thermal transmittance of the composite edge seal for the fabrication of triple vacuum glazing. This value of the thermal conductivity was then used to develop model using finite element method to predict the influence of its wider edge seal and due to its thermal conductivity on the thermal performance.

http://dx.doi.org/10.5772/intechopen.74255

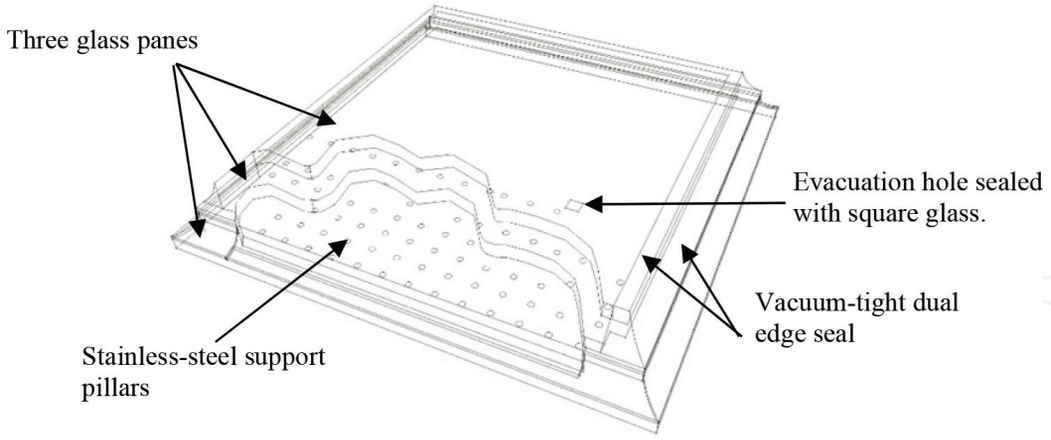

Figure 1. A schematic diagram of vacuum tight dual edge sealed triple vacuum glazing.

2. Methodology

A number of different instruments are available for the measurement of the thermal properties of materials [16]. There are two main methods, steady state method and transient. The steady state approach is further divided into one dimensional heat flow and radial heat flow techniques. One dimensional heat flow technique include the guarded hot plate method which is the ASTM standard based measurement system used for highly insulating materials. The radial heat flow technique includes cylindrical, spherical and ellipsoidal methods. There are a number of transient methods, which can be used for the measurement of thermal conductivity such as hot wire, transient hot strip and transient plane source methods. The experimental measurements of thermal conductivity performed in this study were undertaken using a Hot Disk thermal constants analyser TPS 2500 s. This system is based on the transient plane source (TPS) method. The TPS method consists of a sensor element in the shape of a double spiral which acts both as a heat source to increase the temperature of the sample and a resistance thermometer to record the time dependent temperature increase [17]. In the current experiments, a sensor of design 7577 was used which is made of a 10 μm thick Nickel-metal double spiral. The radius of the sensor was chosen to be 2.001 mm in order to reduce the size of the sample. It is advised [18] that the diameter of the sample should not be less than twice that of the sensor diameter and the thickness of the sample should not be less than the radius of the sensor. The sensor element is usually insulated with a material to provide electrical insulation. The material used is dependent on the operating temperatures. A thin polyamide (Kapton) insulating material was chosen for the sensor insulation which is suitable from cryogenic temperatures to about 500 K [19].

A sensor is placed between two flat cylindrical samples, as shown in **Figure 2**. Passage of a constant electric power through the spiral produces heat, increases the temperature and therefore the resistance of the spiral sensor as a function of time which can be expressed according to Gustavsson et al. [16] as,

$$R(t) = R_o\{1 + \varphi[\Delta T_i + \Delta T_{ave}(\tau)]\} \quad (1)$$

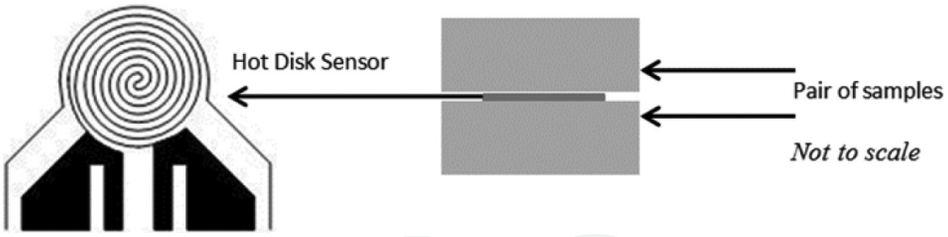

Figure 2. A schematic diagram of the pair of samples and the hot disk sensor placed in between two flat cylindrical samples.

where R_o is the resistance in ohms before the sensor is heated or at time t = 0 s, φ is the temperature coefficient of the resistivity (TCR) of the sensor 7577 i.e. $46.93 \times 10^{-4}\ K^{-1}$, ΔT_i is the initial temperature difference that develops momentarily over the thin insulating layers which cover the two sides of the sensor. The thermal conductivity of the sample can be expressed according to Bohac et al. [19] as,

$$k = \frac{P_o}{\pi^{\frac{3}{2}}.a.\Delta T_{ave}(\tau)}.D(\tau) \tag{2}$$

$$\tau = \sqrt{\frac{t}{t_c}} \tag{3}$$

$$t_c = \frac{a^2}{\alpha} \tag{4}$$

Where α is the thermal diffusivity of the sample in $mm^2\ s^{-1}$. From the experimentally recorded temperature increase over $D(\tau)$ a straight line can be plotted which intercepts ΔT_i, and slope of $\frac{P_o}{\pi^{\frac{3}{2}}.a.\Delta T_{ave}(\tau)}$ which allows the thermal conductivity to be determined. The final straight line from which the thermal conductivity measured is obtained through a process of iteration [17]. During a pre-set time, 200 resistance recordings are taken and from these a relation between temperature and time is established.

3. Results and discussions

3.1. Experimental measurements of the thermal conductivity of the hermetic edge seal

In order to validate the measurements of Cerasolzer allow and J-B Weld epoxy the results were compared with several measurements of the samples of Mild Steel (MSteel) and Indium in four repetitive experiments, combined the cut faces flatten to reduce the experimental errors. The experimental data are plotted in **Figure 3**. As can be seen this work is verified by the reported data of Mild steel and Indium. An increase of temperature with respect to reporting time interval have similar deviations and the highest increase of temperature was recorded for JB-Weld which gives a good agreement with the experimental data. The average

http://dx.doi.org/10.5772/intechopen.74255

temperature increase measured by the TPS sensor type 7577 of the mild steel, indium, J-B Weld epoxy steel resin and Cerasolzer CS186 samples are shown in **Figure 4**. It can be seen that the increase in temperature in the epoxy J-B Weld is greater than the mild steel. This is due to the fact that heat flow in semi-polymeric materials is low compared to metallic materials. The temperature increase in the sample made from Cerasolzer alloy was higher than the indium sample [20, 21].

An average thermal conductivity of a mild steel type SIS2343 sample was measured to be 13.76 Wm^{-1} K^{-1}. The reliability of the measured thermal conductivity is compared with the standard measurement value given in the standard data sheet i.e.13.62 Wm^{-1} K^{-1}. An average thermal conductivity of the indium sample was measured to be 77.84 Wm^{-1} K^{-1} with a repeatability of four times. The thermal conductivity measurement for Cerasolzer alloy and J-B Weld epoxy steel resin, as detailed in **Table 1**, with the deviations were calculated to be ±4 and ±7% in the experimental measurements as compared with the analytical methods as detailed in the Section 2.

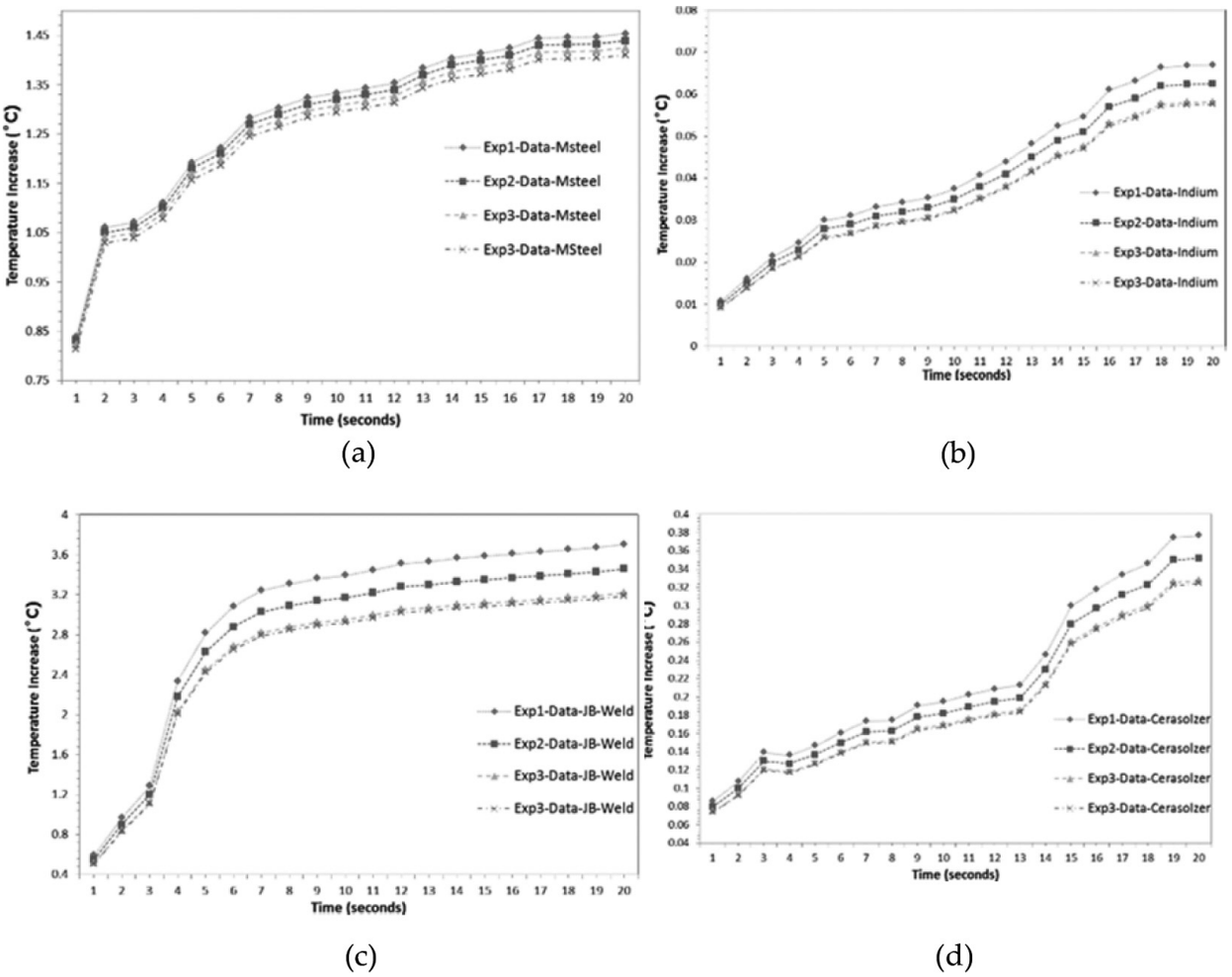

Figure 3. Experimental results as function of temperature increase for JB-weld and Cerasolzer in comparison to the verified mild steel and indium.

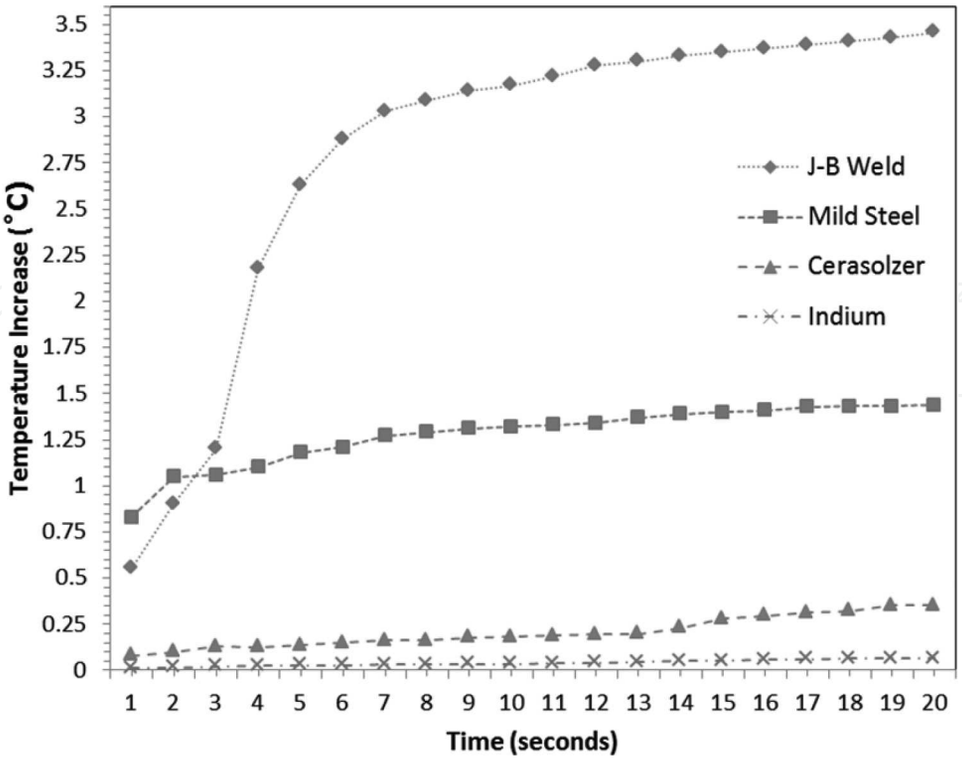

Figure 4. The average recorded temperature increase using the TPS sensor type 7577 for the samples made from mild steel, indium, J-B weld epoxy steel resin and Cerasolzer CS186.

Sample	Thermal conductivity at 21°C (Wm^{-1} K^{-1}) (Deviation)	Measuring time (second)	Power output from sensor (watts)
Mild Steel	13.76 (1%)	20	1
Indium	77.84 (7%)	20	1
Cerasolzer CS186	46.49 (±4%)	20	1
J-B Weld	7.47 (±7%)	20	1

Table 1. Measured thermal conductivities of Cerasolzer alloy CS186 and J-B weld epoxy steel resin and measurements of mild steel and indium.

3.2. Thermal performance analysis of hermetic edge sealed triple vacuum glazing

By utilising the measured thermal conductivities of Cerasolzer alloy as primary seal and JB-Weld as secondary seal, as detailed in **Table 1**, a 3D FE (finite element) model based on a commercial software package MSC Marc was employed to analyse the heat transfer and predict the thermal performance of the triple vacuum glazing. The symmetry of the model was exploited to simulate the heat transfer process in computationally efficient way; only one quarter (150 × 150 mm) of the triple vacuum glazing of dimensions 300 × 300 mm was modelled and simulated using ASTM boundary conditions [22]. Three k glass sheets having thermal conductivity of 1 Wm^{-1} K^{-1} with SnO_2 coatings on inner surfaces with the emissivity

http://dx.doi.org/10.5772/intechopen.74255

of 0.15 were used. The support pillars were incorporated into the model explicitly [23]. This is based on the actual stainless steel pillar array having 16.2 Wm^{-1} K^{-1} of thermal conductivity. The number of support pillars was employed in the triple vacuum glazing that represented by the same number of pillars in the developed finite-element model. Since modelling the pillars with circular cross-section would lead to non-uniform mesh with distorted elements around the pillar, they were modelled using square cross-section (considered the diameter of 0.3 mm, height of 0.15 mm and pillar separation of 24 mm). Additionally, it is already established in the literature that the heat transfer through the pillar does not depend upon its shape but its cross-sectional area under certain boundary conditions [24, 25]. In order to keep the cross-sectional area similar to circular pillar with radius *r,* the side length of each square used is 1.78 *r*. The FE model implemented eight-node iso-parametric elements, with a total of 170,455 elements and 201,660 nodes to represent a quarter of the fabricated triple vacuum glazing. In FE model, the evacuated gap between glasses was represented with as a material with almost zero thermal conductivity to represent triple vacuum glazing. For sake of simplicity, the influence of residual gas among glasses was neglected in the model. In order to achieve realistic results from the simulation, a graded mesh with large number of elements was employed in the pillar. In addition to this, a convergence study was performed on the pillar to ensure the accuracy of the thermal performance predicted using the model. The material properties of the glass sheets applied to the models are those found in [22] and summarised in **Table 2**. The ASTM weather indoor/outdoor boundary conditions were employed in which the indoor and outdoor surface air temperatures were set to be at 21.1°C and −17.8°C respectively in winter conditions [23].

Type	Details	Value
TVG size	Top	284 by 284 by 4 mm
	Middle	292 by 292 by 4 mm
	Bottom	300 by 300 by 4 mm
Glass sheet	Thermal conductivity	1 Wm^{-1} K^{-1}
Surface coating	Three low-e coatings	ε of 0.15 (SnO_2)
Glass sheet support-pillar	Thermal conductivity	16.2 Wm^{-1} K^{-1}
	Material	Stainless steel 304
	Diameter	0.3 mm
	Height	0.15 mm
	Spacing	24 mm
Hermetic edge seal (Primary)	Measured thermal conductivity	46.49 Wm^{-1} K^{-1}
	Material	Cerasolzer CS-186
	Width (wideness)	10 mm
Support seal (Secondary)	Measured thermal conductivity	7.47 Wm^{-1} K^{-1}
	Epoxy steel resin	J-B Weld
	Width (wideness)	4 mm

Table 2. Parameters employed in FEM of the fabricated sample of triple vacuum glazing.

The internal and external surface heat transfer coefficients were set to 8.3 and 30 $Wm^{-2}\ K^{-1}$ respectively [26].

The finite element 3D modelling results show a centre of glass and overall U-value of 0.33 and 1.05 $Wm^{-2}\ K^{-1}$, respectively, this is compared to the predictions of [26] i.e. 0.2 $Wm^{-2}\ K^{-1}$ and [27] i.e. 0.26 $Wm^{-2}\ K^{-1}$ as follows.

The U value (centre of glass) 0.2 $Wm^{-2}\ K^{-1}$ [13] was based on the parametric model of triple vacuum glazing without frame focused on the central glazing area. This value was achieved with 6 mm (top), 4 mm (middle) and 6 mm (bottom) thick untampered soda lime glass sheets having four layers (1-top, 2-middle and 1-bottom) of low-e coatings (ε of 0.03). It is compared with the results of this paper, it is found that an increase of U value (centre-of-glass) 0.13 $Wm^{-2}\ K^{-1}$. Such deviation is due to the design of the fabricated sample reported in this paper which is made of 4 mm(top), 4 mm (middle) and 4 mm(bottom) untampered soda lime glass sheets having three layers of low-e SnO_2 coatings (ε = 0.15). The reason, to use such dimensions and SnO_2 coatings, is the conventional availability of glass sheets from Pilkington Glass and its use in the UK dwelling.

The influence of edge effects is well-detailed in Fang et al. [27, 28] and reported predicted the U values (centre-of-glass and overall) to be 0.26 and 0.65 $Wm^{-2}\ K^{-1}$, respectively. These values were reported for a TVG sample size of 500 × 500 mm with 4 mm (top), 4 mm(middle) and 4 mm (bottom) un-tempered soda lime glass sheets having four layers (1-top, 2-middle and 1-bottom) of low-e coatings (ε of 0.03) with a frame rebate depth of 10 mm and the width of indium-alloy edge seal 6 mm (k of 83.7 $Wm^{-1}\ K^{-1}$). It can be compared, considering all factors, with the results of this paper. It is found that an increase of 0.07 $Wm^{-2}\ K^{-1}$ (deviation of 26.9%) and 0.4 $Wm^{-2}\ K^{-1}$ (deviation of 61.54%) of centre of glass and overall U value, respectively. Such deviations, as per FEM calculations, are due to: the sample size influences to a small extent as the TVG fabricated sample size was of the size 300 × 300 mm, the width of the edge seal influences to a large extent because the TVG fabricated sample width of edge seal used was total 14 mm (10 mm wide Cerasolzer seal and 4 mm wide J-B Weld supportive seal), the use of three SnO_2 low-e coatings (ε of 0.15) in the fabricated sample instead of four Ag low-e coatings (ε of 0.03), and there is no frame rebate depth utilised in the fabricated sample of TVG that has an influence to a small extent on the overall U value of the TVG because the purpose of this paper is focused on the hermetic sealing materials thermal conductivities and triple vacuum glazing area thermal performance only. By accounting all these factors and including the thermal conductivity of the sealing materials, the FEM model predictions are in good agreement.

The simulated isotherms of the triple vacuum glazing for the outdoor and indoor surfaces are shown in **Figure 5**. The mean glass surface temperatures were simulated to be −12.55 and 6.71°C for the outdoor and indoor surfaces of the total glazing area. The mean surface temperatures for the centre of glass area were simulated to be 16.43 and −16.60°C for the outdoor and indoor surfaces respectively. It can be seen the temperature discrepancies on the outdoor side are smaller than the indoor side. This is, however, due to the use of 14 mm composite edge seal as compared to the edge seal thickness of 6 mm [28]. Thus, the edge effects need to be reduced by narrowing the width of edge-seal to 9 mm (6 mm and 3 mm for primary and secondary respectively) which reduces the centre-of-glass U-value of 0.043 $Wm^{-2}\ K^{-1}$.

http://dx.doi.org/10.5772/intechopen.74255

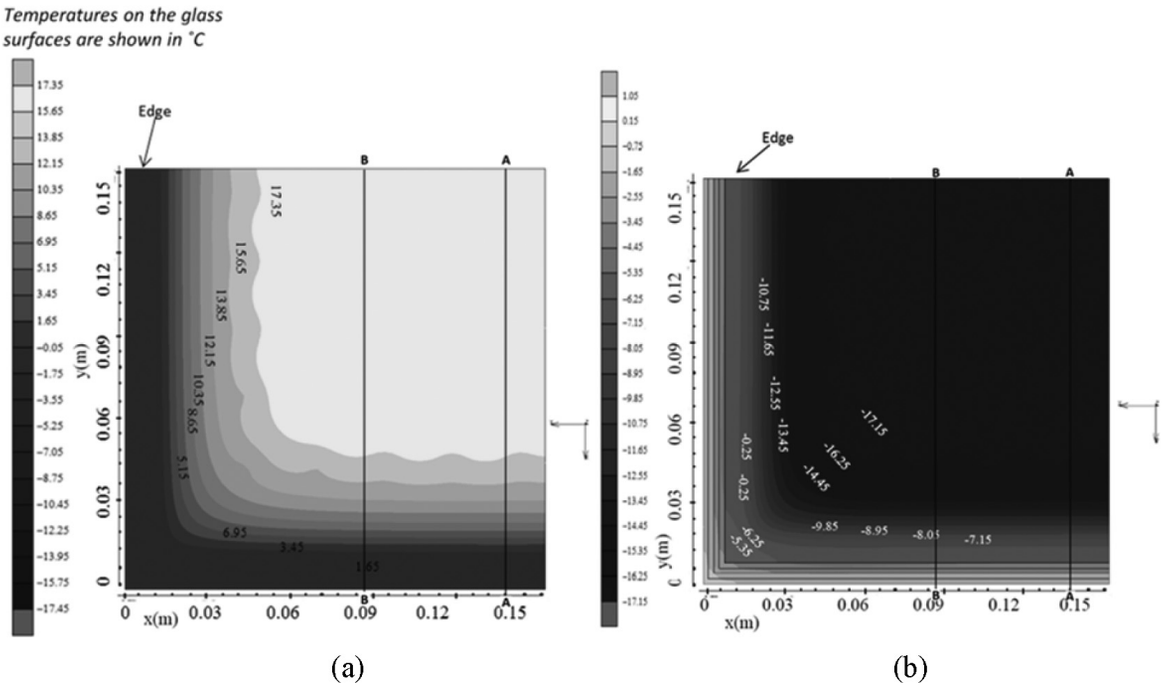

Figure 5. The FEM based isotherms on (a) the indoor (b) the outdoor glass surface showing the temperature variations from the edge area towards the central glazing area.

A finite element calculations of the temperature loss due to a wider edge seal are analysed, along the outer surface lines AA and BB (as shown in **Figure 5**), showing the temperature gradient from the glazing edge to the central area of the glazing as illustrated in **Figure 6**. An

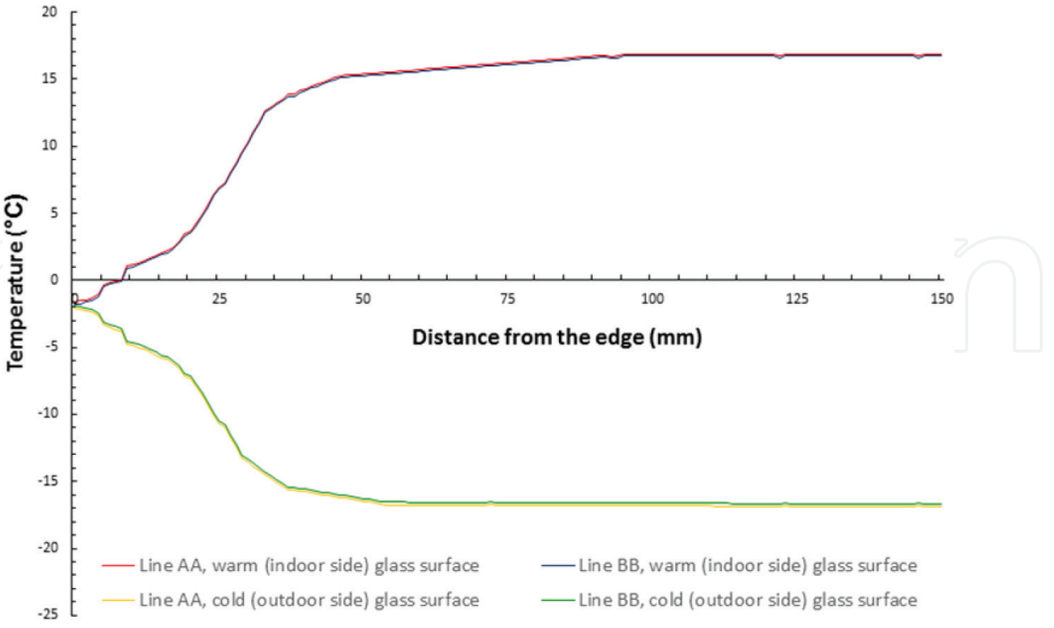

Figure 6. The temperature loss, due to a wider edge seal, along the glazing surface lines AA and BB showing the temperature gradient from the glazing edge to the central area of the glazing of the one quarter of total sample of 300 × 300 mm using ASTM boundary conditions.

influence of wider edge seal on temperature loss around the edge area has affected the centre-of-pane U value. **Figure 6** shows there are smaller temperature gradients on the cold surface as compared to the warm surface of the glazing which is due to the periodic shape of the edge sealing area of triple vacuum glazing as shown in **Figure 1(b)**. It can be seen the influence of temperature gradient loss spread to 54 and 84 mm on the cold and warm side respectively. When comparing with the temperature gradient profiles of [26, 27] the results are in good agreement with the results presented in this paper.

4. Conclusions

In this study, a hot disk thermal constants analyser TPS 2500s using transient plane source technique with a sensor element in the shape of double spiral and resistance thermometer is proved to be an adequate in measuring and analysing the thermal conductivity of hermetic edge sealing materials (i.e. Cersolzer CS186 and J-B Weld). The technique was validated by measuring the thermal conductivity for Mild Steel and Indium and comparing these results with those available in literature. This validated technique based on hot disk thermal constants analyser was then used to measure thermal conductivity of Cerasolzer CS186 alloy and J-B Weld epoxy steel resin and found to be 46.49 and 7.47 Wm^{-1} K^{-1}, respectively. It has been shown that an increase in temperature has direct relation with respect to reporting time with highest increase in temperature was recorded for JB-Weld for a given time period, which is in agreement with the experimental data. It has also been shown that the increase in temperature in the epoxy J-B Weld is greater than that of mild steel. This observation is linked to the fact that the heat flow in semi-polymeric materials is less as compared to that of metallic materials. The temperature increase in the sample made from Cerasolzer alloy was higher than that of indium sample. These values were utilised for the numerical prediction of thermal performance of triple vacuum glazing using 3D FE model. The simulated resulted showed that the centre-of-glass and total U-value of 300 $\times$ 300 mm triple vacuum glazing are 0.33 and 1.05 Wm^{-2} K^{-1}, respectively. The thermal transmittance values can be reduced by using soft low emittance coatings and by reducing the width of the hermetic edge seal to 9 mm. An influence of wider edge seal on temperature loss spreading from the edge to the central glazing area was further analysed with the FEM model calculations. In which it is concluded that the wider edge seal has affected the U-value to 0.043 Wm^{-2} K^{-1} because of the temperature gradient loss spread to 54 and 84 mm on the cold and warm side respectively.

Acknowledgements

The author acknowledge the valuable advice and guidance received from Prof P. C. Eames during the course of this research work. This work was supported by the EPSRC funded project CALEBRE (Consumer Appealing Low energy Technologies for Building Retrofitting) [EP/G000387/1].

http://dx.doi.org/10.5772/intechopen.74255

Nomenclature

a	overall radius of the sensor [m]
d	thickness of the glass sheet [mm]
D	dimensionless time dependent variable
k	thermal conductivity [$Wm^{-1} K^{-1}$]
P_o	total output power from the sensor [W]
R	resistance [ohms]
t	time [s]
ΔT_i	initial temperature difference [K]
$\Delta T_{ave}(\tau)$	average temperature increase of the sample surface on the other side of the sensor [K]
T	temperature [°C]
U	thermal transmittance [$Wm^{-2} K^{-1}$]

Abbreviations

ASTM	American Society for Testing and Materials
CALEBRE	consumer appealing low energy technologies for building retrofitting
CIBSE	chartered institution of building services engineers
FEM	finite element model
TPS	transient plane source
TVG	triple vacuum glazing

Subscripts

ave.	average
o	before the sensor is heated at
c	t = 0 s characteristic

Greek letters

ρ	density [kgm^{-3}]
α	thermal diffusivity of the sample [$mm^2 s^{-1}$]

τ dimensionless time dependent function

φ temperature coefficient of the resistivity [K^{-1}]

ϕ heat loss [W]

ε emittance

Author details

Saim Memon

Address all correspondence to: s.memon@lsbu.ac.uk

Centre for Advanced Materials, Division of Electrical and Electronic Engineering, School of Engineering, London South Bank University, London, UK

References

[1] Memon S, Eames PC. Heat load and solar gain prediction for solid wall dwellings retrofitted with triple vacuum glazing for selected window to wall area ratios, World Renewable Energy Forum, WREF 2012, Including World Renewable Energy Congress XII and Colorado Renewable Energy Society (CRES) Annual Conference, Colorado, USA. 6, 2012. pp. 4636-4643. ISBN: 9781622760923

[2] Memon S, Eames PC. Predicting the solar energy and space-heating energy performance for solid-wall detached house retrofitted with the composite edge-sealed triple vacuum glazing. Energy Procedia. 2017;**122**:565-570. DOI: 10.1016/j.egypro.2017.07.419

[3] Memon S. Analysing the potential of retrofitting ultra-low heat loss triple vacuum glazed windows to an existing UK solid wall dwelling. International Journal of Renewable Energy Development. 2014;**3**(3):161. DOI: 10.14710/ijred.3.3.161-174

[4] Memon S. Design, fabrication and performance analysis of vacuum glazing units fabricated with low and high temperature hermetic glass edge sealing materials. [PhD Thesis]. UK: Loughborough University Institutional Repository; 2013. DOI: https://dspace.lboro.ac.uk/2134/14562

[5] Fang F, Eames PC, Norton B, Hyde TJ. Experimental validation of a numerical model for heat transfer in vacuum glazing. Solar Energy. 2006;**80**:564-577. DOI: 10.1016/j.solener.2005.04.002

[6] Benson DK, Tracy CE. Evacuated window glazings for energy efficient buildings. Proceedings of SPIE 0562, Optical Materials Technology for Energy Efficiency and Solar Energy Conversion IV. San Diego, CA; 1985. p. 250

[7] Eames PC. Vacuum glazing: Current performance and future prospects. Vacuum. 2008; **82**:717-722. DOI: https://doi.org/10.1016/j.vacuum.2007.10.017

[8] Robinson SJ, Collins RE. Evacuated windows—theory and practice. ISES Solar World Congress, International Solar Energy Society, Kobe, Japan; 1989

[9] Collins RE, Simko TM. Current status of the science and technology of vacuum glazing. Solar Energy. 1998;**62**:189-213. DOI: 10.1016/S0038-092X(98)00007-3

[10] Collins RE, Tang JZ, Merrylands. Design improvements to vacuum glazing. 1999. US Patent No. 5891536

[11] Griffiths PW, Di Leo M, Cartwright P, Eames PC, Yianoulis P, Leftheriotis G, Norton B. Fabrication of evacuated glazing at low temperature. Solar Energy. 1998;**63**:243-249. DOI: 10.1016/S0038-092X(98)00019-X

[12] Zhao JF, Eames PC, Hyde TJ, Fang Y, Wang J. A modified pump-out technique used for fabrication of low temperature metal sealed vacuum glazing. Solar Energy. 2007;**81**:1072-1077. DOI: 10.1016/j.solener.2007.03.006

[13] Manz H, Brunner S, Wullschleger L. Triple vacuum glazing: Heat transfer and basic mechanical design constraints. Solar Energy. 2006 Dec 31;**80**(12):1632-1642. DOI: https://doi.org/10.1016/j.solener.2005.11.003

[14] Memon, S. Investigating energy saving performance interdependencies with retrofit triple vacuum glazing for use in UK dwelling with solid walls, Sustainable Development on Building and Environment: Proceedings of the 7th International Conference, Reading, UK; 2015. ISBN-13: 978–0993120701

[15] Memon S, Farukh F, Eames PC, Silberschmidt VV. A new low-temperature hermetic composite edge seal for the fabrication of triple vacuum glazing. Vacuum. 2015;**120**:73-82. DOI: 10.1016/j.vacuum.2015.06.024

[16] Gustavsson M, Karawacki E, Gustafsson SE. Thermal conductivity, thermal diffusivity, and specific heat of thin samples from transient measurements with hot disk sensors. Review of Scientific Instruments. 1994 Dec;**65**(12):3856-3859. DOI: https://doi.org/10.1063/1.1145178

[17] Gustafsson SE. Transient plane source techniques for thermal conductivity and thermal diffusivity measurements of solid materials. The Review of Scientific Instruments. 1991 Mar;**62**(3):797-804. DOI: 10.1063/1.1142087

[18] Hot Disk Thermal Constants Analyzer. 2013. TPS 2500s Instruction Manual, Mathis Instruments. [Accessed: 05–07-2013]

[19] Bohac V, Gustavsson MK, Kubicar L, Gustafsson SE. Parameter estimations for measurements of thermal transport properties with the hot disk thermal constants analyzer. The Review of Scientific Instruments. 2000 Jun;**71**(6):2452-2455. DOI: 10.1063/1.1150635

[20] Memon S, Eames PC. An investigation on edge sealing materials for the fabrication of vacuum glazing, 3rd School of Electrical, Electronic and Systems Engineering (EESE) Research conference, 2013 Mar 21–22, Loughborough University, UK

[21] Memon S. Experimental measurement of hermetic edge seal's thermal conductivity for the thermal transmittance prediction of triple vacuum glazing. Case Studies in Thermal Engineering. 2017;**10**:169-178. ISSN 2214-157X. DOI: 10.1016/j.csite.2017.06.002

[22] ASTM, Standard procedures for determining the steady state thermal transmittance of fenestration systems, ASTM Standard E 1423-91, in: 1994 Annual Book of ASTM Standard 04.07, American Society of Testing and Materials; 1991. pp. 1160-1165

[23] Memon S, Farukh F, Eames PC, Silberschmidt VV. A new low-temperature hermetic composite edge seal for the fabrication of triple vacuum glazing. Vacuum. 2015;**120**:73-82. DOI: 10.1016/j.vacuum.2015.06.024

[24] Collins RE, Robinson SJ. Evacuated glazing. Solar Energy. 1991 Jan;**47**(1):27-38. DOI: 10.1016/0038-092X(91)90060-A

[25] Wang J, Eames PC, Zhao JF, Hyde T, Fang Y. Stresses in vacuum glazing fabricated at low temperature. Solar Energy Materials & Solar Cells. 2007;**91**(4):290-303. DOI: 10.1016/j.solmat.2006.10.007

[26] Fang Y, Hyde T, Hewitt N, Eames PC, Norton B. Comparison of vacuum glazing thermal performance predicted using two-and three-dimensional models and their experimental validation. Solar Energy Materials & Solar Cells. 2009;**93**(9):1492-1498. DOI: https://doi.org/10.1016/j.solmat.2009.03.025

[27] Fang Y, Hyde TJ, Hewitt N. Predicted thermal performance of triple vacuum glazing. Solar Energy. 2010;**84**(12):2132-2139. DOI: 10.1016/j.solener.2010.09.002

[28] Fang Y, Hyde TJ, Arya F, Hewitt N, Wang R, Dai Y. Enhancing the thermal performance of triple vacuum glazing with low-emittance coatings. Energy and Buildings. 2015;**97**:186-195. DOI: 10.1016/j.enbuild.2015.04.006